Hindawi
Journal of Engineering
Volume 2024, Article ID 5540010, 19 pages
https://doi.org/10.1155/2024/5540010

*Research Article*

# Modelling and Output Power Estimation of a Combined Gas Plant and a Combined Cycle Plant Using an Artificial Neural Network Approach

**Vasileios Xezonakis,[1] Olusegun David Samuel ,[1,2] and Christopher Chintua Enweremadu [1]**

[1]*Department of Mechanical Engineering, University of South Africa, Science Campus, Private Bag X6, Florida 1710, South Africa*
[2]*Department of Mechanical Engineering, Federal University of Petroleum Resources, Effurun, P.M.B 1221, Warri, Delta State, Nigeria*

Correspondence should be addressed to Christopher Chintua Enweremadu; enwercc@unisa.ac.za

Received 9 June 2023; Revised 31 January 2024; Accepted 13 April 2024; Published 6 May 2024

Academic Editor: Angelo Maiorino



Artificial neural networks (ANNs) have gained prominence among contemporary computing techniques due to their capacity to handle complicated stochastic datasets and nonlinear modelling in combined gas and combined cycle power (COGAS) plants. Researchers, academicians, and stakeholders have been unable to predict, ensure effective operation, and prevent power outages in COGAS due to the nonlinearity. The first implementation of the simultaneous adoption of three types of ANNs using Levenberg–Marquardt (LM), Bayesian regularisation (BR), and scaled conjugate gradient (SCG) configurations for training and assessing a combined cycle power plant output is presented. The dataset used in this research is a 9568-unit full combined cycle power plant basis load dataset, accessible through the public UCI Machine Learning Repository. It incorporates ambient temperature, exhaust vacuum, ambient pressure, and relative humidity as input parameters to predict the electric output power. The most accurate and dependable electric power predictions could be identified for 70% of the total data, of which 6698 were trained, 15% were tested, and 15% were validated (2870). By using the three training techniques, namely, LM, BR, and SCG, the parameterized networks are studied, increasing the number of hidden layers from 20 to 500. The lowest root-mean-square error value for a multilayer perceptron (MLP) architecture is 3.631%, which is lower than the values of 4.17%, 4.35%, and 4.63% for comparable MLP structures (20 to 500), documented in the literature. The LM and BR algorithms outperform SCG. These adopted algorithms could be a cutting-edge application in the power plant industry and other real-world applications for reliable solutions, to satisfy emerging societal needs with environmental benefits.

## 1. Introduction

The production and consumption of many energy types, especially electricity, heat, and chemicals, are very necessary for each nation's economic development. The primary source type of the area of concern in this regard is electricity. Traditional and hybrid power plants implement an assortment of fossil fuels and energy sources to produce electricity. To generate electricity, power plants employ a variety of renewable energy sources, including hydroelectric, solar, and wind. The variety of thermal power plant stations has recently declined for several reasons, including increasing capital prices, installation challenges, and resource availability. Consequently, active plants currently produce 65% of the world's energy despite having a negative influence on the environment [1].

The forecasting of thermal power plant parameters using artificial intelligence (AI) has captured the attention of researchers across the globe. Because of their similarity and ease of use, ANNs have been the pioneers among artificial intelligence systems [2]. Modelling has been a reliable correlation due to the varied design conditions of the thermodynamic input factors vs. response, specifically in power estimation [3]. Owing to their limited processing capacity and ability to represent human-brain interactions, McCullogh and Pitts [4] were the first to introduce neural networks.

Cutting-edge technology with exceptional capabilities and extensive energy field implementations is used in modern, upgraded approaches for energy production. Aside from the thermodynamic analysis, these approaches entail the adaptation of fuzzy logic and neural networks, and they provide engaging responses.

Numerous studies have emphasized the use of conventional thermodynamic analysis to evaluate the power and energy efficiency of various kinds of power plants.

Mohammed [5] gave an overview of optimisation techniques for enhancing the efficiency of a combined cycle power plant. According to Samani [6], the ANN model is effective at accurately predicting a plant's power production. Yoru et al. [7] employed ANN to simulate an exergetic-based cogeneration system and reported that it can determine the system's exergetic indices.

However, due to their exceptional features such as improved fuel conversion performance for identical energy produced and less fuel consumption with a positive impact on the environment for the benefit of society, alternative combined types of plants (CCPP and COGAS) have rapidly expanded in recent years to replace conventional power plants for power generation. Nevertheless, they present the shortcoming of not improving their expensive energy prices, which is more applicable. COGAS plants are applied to ship propulsion extensively with optimum efficiency and the ability to handle troubleshooting issues, as well as maintenance patterns [8].

Adaptation of novel machine learning methodology towards the output power prediction in combined types of power plants is very popular. An interesting comparison of the logistic regression (LR), and the traditional MLP architectures, indicates the advocacy of random forest networks using optimum regression values [9]. A continuous conditional random field model contributes to this direction by improving the power plant's performance based on mean squared error (MSE) significantly, compared with regression trees and neural network techniques [10]. Implementation of a genetic multilayer perceptron algorithm forecasts higher accurate power outcomes, compared with linear regression and pace regression methodologies [11].

A new methodology of a grid search optimised stacked ensemble machine learning algorithm with optimum performance compared with the random forest and the vote ensemble is identified [12]. A gradient-based generalized additive model provides optimum performance measures that benefit the plant's consistency and its financial performance [13]. The incorporation of simpler learning algorithms instead of the combined deep machine learning algorithms and neural networks with optimum outcomes at the lowest computational cost is proposed [14, 15]. The main configuration and the operational attributes of a combined cycle power plant will be explained briefly in the methodology section.

There is an underlisted literature evaluation of the artificial intelligence methodology with interesting results in the power plant sector and additional positive qualities.

## 2. Literature Review

ANNs are assumed to be an efficient approach to handle complex and ill-defined problems; therefore, they are adopted by many researchers for different real-world engineering applications, such as in the solar sector [16] and solar power impact on islands [17]. Energy prediction in solar power plants has been investigated as well [18]. In the power plant sector, various models for many input and output datasets have been proposed over the last few years with reliable results. A CCPP's power output has been modelled and its fidelity outcomes have been approximated, based on different thermodynamic input parameters [19].

A comparison between various machine learning methods to predict the output energy of a basic load operation has been proposed by Tufekci [20]. The validity and reliability of neural networks in a traditional gas turbine power plant, in terms of ambient temperature impact on power generation and fuel consumption, are highlighted [21]. A modelling analysis in a single-shaft gas turbine resulted in encouraging outcomes [22]. The control and performance analysis of a combined heat and power plant has been studied by Kaiadi [23]. An interesting application of neural networks via the CHP plant to microgas turbines with encouraging outcomes was proposed [24]. A combined cycle plant control technique using a linearisation model technique was highlighted [25].

A novel methodology for the prediction of the electric power output, with an optimised matching algorithm and encouraging times, was investigated [26]. The monitoring of the drum level of a thermal power plant, adopting a back-propagation neural network method was achieved [27]. Another application of artificial intelligence (AI) is found in a combined cooling, heating, and power plant, using various input parameters without including the fuel gas characteristics, to predict its performance [28].

An efficiency of more than 60% was achieved by modelling a COGAS power plant using the multilayer perceptron network design [29]. In the construction sector, distributed energy resources have been studied through various neural network topologies for the evaluation of a classified pattern of a combined heat and power plant [30]. The heat rate is incorporated as an output parameter using three input parameters, including the fuel gas heat rate (P1), the $CO_2$ percentage (P2), and the power output (P3), for the training/evaluation processes. This combination and the absence of the input parameters (P1, P2, and P3) achieved an improved heat rate with an assigned regression value of 0.995 [31].

A simulation of the transient performance with encouraging results was found [32]. The monitoring and diagnosis of a combined heat and power plant have been researched on with the aid of a neural network [33]. The efficiency of an industrial gas turbine plant through neural networks considering four input thermodynamic parameters is forecasted after 10,000 epochs [34]. The modelling of the hourly electrical output power of a COGAS plant via neural networks involving various input parameters by improving the twofold approach and the mean squared error by 3.176 and 0.99675 was performed [35]. The failure rate in the power equipment prediction for a number of input variables affects its performance [36]. Another application of the ANNs is found in the modelling of an industrial oil-fired boiler plant with reliable results [37].

In the gas turbine field, the performance map of a compressor has been predicted and the noise reduction in the measured data has been achieved via neural networks, thus improving their operational quality [38]. In a steel thermal plant with implicated input variables, ANN efficiency is superior to the autoregressive moving average exogenous time-series model [39]. In a CCHP, the exergy efficiency, the overall exergy destruction rate, and the performance prognosis are predicted with accurate results. The financial development and the planning of a coupled power network are optimised with the assistance of neural networks. The short-term load prediction in power plants is highlighted. A hybrid model consisting of a fuzzy logic exergy model and a neural network of a CHP system provides a reliable performance [40].

The overall performance prediction in a western Balkan power plant with controlled modifications was proposed [41]. A comparison between the multilayer perceptron (MLP) and the radial basis function (RBF) networks has been explored for indicating the fault analysis of gas turbines, indicating their outperformance [42]. Additionally, the application of neural networks to reduce unusual (indirect) losses in a thermal power plant is proposed [43]. Another approach forecasts the performance of a traditional thermal power plant and certifies reliable experiments by considering minimal error and robust outcomes. An alternative method for simulating thermodynamic systems, applied to power plants, using machine learning and soft computing approaches led to precise output power outcomes [44]. A hybrid model consisting of an ANN and a generic algorithm that selects the optimum architecture via the trial-and-error process, improving the computational cost, is presented [45].

Adaptation of various deep learning methods, such as single and fast neural networks, has been implemented for the electric power estimation of a combined cycle power plant with the highest accuracy, at a minimum computational cost [46].

A statistical inference predictive performance model with outstanding outcomes and cost benefits in the entire process has been identified by Dutta and Ghosh [47]. A study by Kaewprapha et al. [48] reported the monitoring process of a combined power plant optimised via the incorporation of machine learning estimators. A multilinear regression machine learning methodology for optimum predictive load estimator is acknowledged [49]. A forecasting model and a decision-making tool of coherent complex data optimum environmental control via artificial intelligence have been validated successfully [50].

Wang et al. [51] have developed a hybrid optimisation method between the butterfly optimisation algorithm and the support vector regression model. This was used to estimate the electric power accurately, thereby avoiding local optimisation outcomes. A sensitivity analysis of the interpreted neural network tool, including various agnostic models, provides influential and efficient results for full operating conditions [52]. In the CCGT, an interesting investigation of control optimisation of its auxiliary components was carried out, through deep learning methodologies [53]. A metaheuristic optimisation algorithm, coupling a novel neural network with an electrostatic discharge optimiser, enhances robust solutions [54]. A brief introduction on the closure of the gaps leading to contribution to knowledge as well as the aims of the present study is depicted therein.

## 3. Motivation, Gaps in Knowledge, and Aim of Study

In this study, the main interest is devoted to COGAS and the CCPPs with the main aim being to model and predict the performance of this type of plant using a neural technique for multidimensional data (9568) of a full CCPP basis load in Turkey [55]. Therefore, four input parameters such as ambient temperature, exhaust vacuum (V), ambient pressure, and relative humidity are used to forecast the electric output power (EP).

Table 1 highlights the application of AI tools in different types of combined power plants. As observed, many tools have been used to predict and model the CCPP and COGAS plant, and the choice and suitable solicitation of leading-edge tools, precisely AI-based extrapolative models, capable of simulating nonlinear trends in the combined plant, have not yet been copiously reconnoitred. It is based on this premise that this study implemented an MLP network structure of artificial neural network (ANN), which is more robust and reliable on the massive dataset (9568) using the key findings to make a comparison with the previous studies [3, 5, 20]. To the best of the author's knowledge, power plant modelling and analysis have not fully and appropriately used the MLP network. The new approach is used to address the problem of multidimensional handling of the full dataset to close the knowledge gap effectively, prevent power outage, and stabilize its operation. The methodology, including the operational characteristics of the COGAS plant and the main aspects of the MLP architectural model of the current investigation, is described in the following section.

## 4. Methodology

In the current study, the proposed COGAS operational diagram with its functional competencies will be used for the novel estimation of the electric output power and the overall performance. Therefore, as shown in Figure 1 and thoroughly explained elsewhere [20], it is made up of a gas turbine, a steam turbine, and a heat recovery steam generator (HRSG).

Table 1: Overview of AI-based modelling tools on assorted power plants.

| Types of plant | Plants' decision parameters | AI-based modelling tools | Responses | Remarks on deficiency | Findings | References |
|---|---|---|---|---|---|---|
| Combined cycle power plant | Ambient temperature, vacuum, ambient pressure, relative humidity | Machine learning approaches (MLAs) | CCPP hourly electric output power prediction | Various MLAs such as the K-nearest neighbours (KNN), gradient-boosted regression rate (GBRT), linear regression (LR), artificial neural networks (ANN), and deep neural networks (DNN), estimate the electric power output with significant outcomes | Results show that the state-of-the-art outperformance of GBRT in terms of optimum electric output power solutions is depicted | Siddiqui et al. [15] |
| Combined cycle power plant | Ambient temperature, vacuum, ambient pressure, relative humidity | Machine learning approaches (MLAs) | Power plant's electrical power output | MLPRM was not accosted in predicting the power output of the plant | Results show that the bagging REP tree method is the most suitable among the MLAs | Tüfekci [20] |
| Combined cycle power plant | Ambient temperature, vacuum, ambient pressure, relative humidity | Hybrid machine learning approaches | Power plant's electrical power output with less waste | Butterfly optimisation algorithm (BOA) combined with a *Phasmatodea* population evolution (PPE) algorithm (BOAPPE), jointly with the support vector machine (SVM) predicted accurately the power output of CCCP | Results show that the BOAPPE strategy improved the convergence speed and avoided trapping into local optimum outcomes | Wang et al. [51] |
| Combined cycle gas turbine power plant | Ambient temperature, vacuum, ambient pressure, relative humidity | ANN-electrostatic discharge algorithm (EDA): ANN-EDA | Power plant's electrical output power prediction | The multilayer perceptron regression method (MLPRM) was not adopted in the modelling of their plant | The reliability of prediction of power electricity by SDA-ANN established | Zhao and Kok Foong [54] |
| Combined cycle gas turbine power plant | Inlet flue temperature, absorber column operating pressure, amount of exhaust gas recycled, and amine concentration | Taguchi's design of the experiment | Optimisation of postcombustion $CO_2$ capture | Monoethanolamine solvent, employed via Taguchi's design experimental method, mitigated the energy demands of the system | The statistical optimisation concept of the postcombustion capturing of $CO_2$ is demonstrated | Alexanda Petrovic and Masoudi Soltani [56] |

Table 1: Continued.

| Types of plant | Plants' decision parameters | AI-based modelling tools | Responses | Remarks on deficiency | Findings | References |
|---|---|---|---|---|---|---|
| Natural gas-fired combined cycle power plant | Flue gas emission dataset between 2011 and 2015 | Hybrid machine learning method | Power plant's NOx emission prediction | ANFISGA model predicted accurately the NOx emissions at the minimum error | Results show that the impact of the genetic algorithm (GA) on ANFIS performance towards optimum solutions | Dirik [57] |
| Gas turbine combined cycle power plant | Dynamic optimal set point for the regularisation level | Hybrid machine learning approaches | Power plant's performance prediction | A fuzzy logic model (FL) coupled with a genetic algorithm (GA) predictive supervisory controller predicted accurately the performance of the power plant | Results show that the hybrid fuzzy GA predictive controller captures the system's nonlinearities with optimum performance solutions | Saez et al. [58] |
| Combined cycle power plant boiler | Input data are selected via a sensitivity analysis approach | Machine learning approaches (MLAs) | CCPP boiler performance | A cluster number of optimum Taguchi–Sugeno fuzzy logic (FL) models, derived accurately the performance of the CCPP | Results show the economic optimisation of the plant's performance with the nonlinear FL model and the superheated steam pressure via the linear model FL | Sáez and Zuñiga [59] |

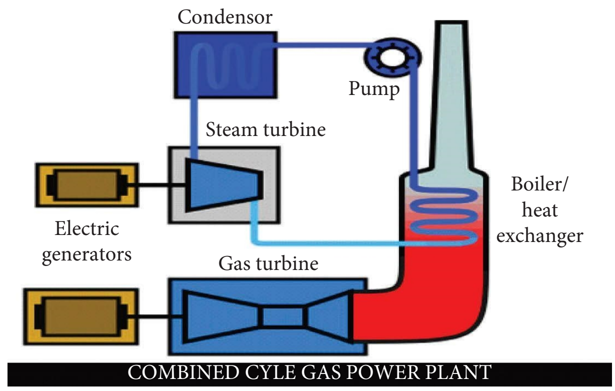


Figure 1: COGAS power plant diagram [20].

*4.1. Operation of COGAS.* The following steps are involved in the operation of the COGAS power plant:

(i) The fuel burns on the gas turbine so that the turbine blades spin and drive the electricity generators

(ii) The HRSG captures the exhaust heat from the gas turbine, creating a stream from the gas turbine exhaust and delivering it to the steam turbine

(iii) The steam turbine uses the steam delivered by the HRSG to generate additional electricity driving an electricity generator

The collected data (9568) are obtained from actual and reliable full basis measurements from a 210 MW power capacity in Turkey for the period from 2006 to 2011. The preprocessing phase of modelling the numerical data is presented in Table 2. The data information for the inlet and outlet phases of a sample population of 9568 actual data includes the ambient temperature, the exhaust vacuum (V, cmHg), the ambient pressure, and the relative humidity (RH), while the output parameter is the electric power (EP) in MW. This population set will be split into the training and testing portions, via the Neural Network Toolbox in the MATLAB environment.

*4.2. Development of the Multilayer Perceptron (MLP) for the Plant.* Using the Neural Network Toolbox in the MATLAB environment, this population set will be split into training and testing parts. As shown in Figure 2, an artificial neural network (ANN) is made up of several parallel processing, networked adaptable units, or neurons. The multilayer perceptron (MLP) architecture at the hidden layer is visible when there is more than one neuron. Using an applied transfer function (activation function) to collect input values from the input layer, the MLP learns to predict the final output information (electric power (EP)) by sending its outputs to the neurons in the output layer.

There are different activation function types such as the *logsigmoid (logsig)* and the *tansig* with different attributes. Both activation functions portray the input values within a range from 0 to 1. The logsig generates output as the neuron's net input goes from negative infinity to positive infinity, and its expression and its characteristic response are illustrated in the following equation and Figure 3, respectively:

$$f(x) = \frac{1}{1 + e^{-x}}. \tag{1}$$

Identically, the tansig's hyperbolic tangent is a training function that calculates a layer's output from its net input. Its expression and its characteristic response are provided in (2) and Figure 4. Tansig is adopted in this study to get more accurate results.

$$f(x) = \frac{2}{1 + e^{-2x}} - 1. \tag{2}$$

*4.3. Methods for the MLP of the ANNs.* Electric power is the output variable, and the four input factors (features) that are taken into account by ANNs as the primary modeller are (i) ambient temperature, (ii) exhaust vacuum, (iii) ambient pressure, and (iv) relative humidity. The entire set of samples (9568) was divided into training, testing, and validation sets over a six-year period (2006–2011). As a result, given limited CPU requirements, 70% are trained, 15% are tested, and 15% are validated for the network's performance in terms of the lowest RMSE value.

*4.3.1. Architectural Model.* Figure 5 depicts the proposed testing, training, and validation procedure for the 1000 validation steps and the three different training algorithms (LM, BR, and SCG) employed in the current test scenario with 10,000 epochs.

The architecture of the ANN, which comprises the number of neurons, layers, training functions, and learning algorithms, is used to construct the network. The study comprises the automatic adoption of the neural network architecture created using the graphical user interface (GUI) features of MATLAB software. Additional investigation was made to amend the dataset percentage in terms of training/testing/validation without achieving more accurate outcomes. The input and target data are provided, and the weight biases are adjusted to align the targets with the actual

Table 2: Sample real data of the combined cycle power plant [55].

| Sample | AT (input) (°C) | V (input) (cmHg) | AP (input) (mbar) | RH (input) | EP (output) (MW) |
|---|---|---|---|---|---|
| 1 | 9.34 | 40.77 | 1010.94 | 90.01 | 490.48 |
| 2 | 23.64 | 59.49 | 1011.42 | 74.23 | 445.75 |
| 3 | 29.74 | 56.91 | 1007.15 | 41.91 | 439.76 |
| 4 | 19.07 | 49.69 | 1007.22 | 76.79 | 452.09 |
| 5 | 11.84 | 40.66 | 1017.12 | 97.23 | 464.43 |
| ... | ...... | ...... | ...... | ...... | |
| 9565 | 16.65 | 49.69 | 1014.01 | 91.04 | 460.03 |
| 9566 | 13.19 | 39.18 | 1023.67 | 66.78 | 469.62 |
| 9567 | 31.32 | 74.33 | 1012.92 | 36.48 | 429.57 |
| 9568 | 24.48 | 69.45 | 1013.86 | 62.39 | 435.74 |

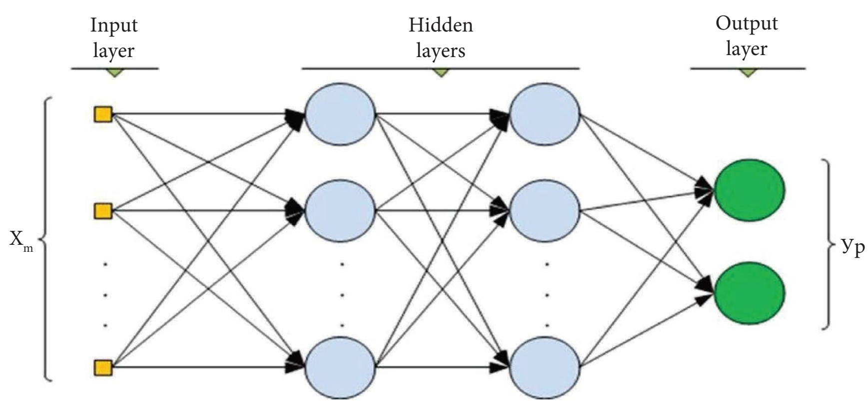


Figure 2: ANN configuration with input, hidden (MLP), and output layers [20].

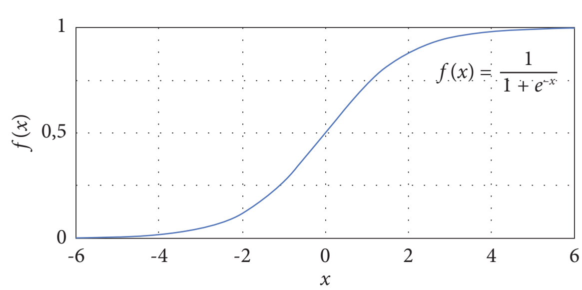


Figure 3: Characteristic response of the logsig activation function [60].

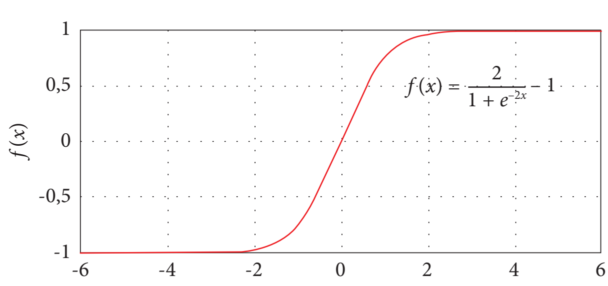


Figure 4: Characteristic response of the tansig activation function [60].

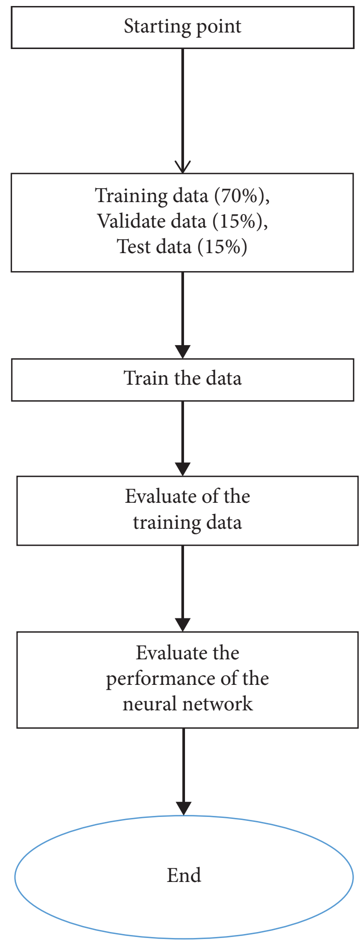


FIGURE 5: Architecture of the flowchart process.

data. In addition, three training methods are chosen based on the MATLAB Neural Network Toolbox's capabilities. The network's database's testing process and performance are investigated via the mean squared error, according to the long-term multidimensional forecasted data. The implementation of the mean bias error (MBE) simultaneously shows the deviation between the predicted data and the actual data but is not considered. Therefore, the reliability of the network's performance only depends on the MSE. The structure of the network, designating the four input parameters with the hidden layers (1) and the output layer, is presented in Figure 6, while the reliable and interesting outcomes with their physical interpretation are discussed in the following section.

## 5. Results and Discussion

This section highlights the findings and their analysis as well as some conclusions regarding their relevance. Due to the network's bias and random beginning weights, the training process using the settings for the full dataset produces different results for each simulation. The real data are split into three categories: training (70%), validation (15%), and testing (15%). Table 3 illustrates these settings for the respective number of runs.

The subsequent subsections address the use and examination of the Neural Network Toolbox through the GUI features of the Input/Output fitting tool in MATLAB R2018b [61]. This approach involves the comparison of three alternative training methods, namely, scaled conjugate gradient, Levenberg–Marquardt, and Bayesian regularisation. The theoretical study of these methods' theoretical foundation is excluded, and further details are available in the literature.

*5.1. Levenberg–Marquardt Training Algorithm.* Figure 2, which is depicted in the previously mentioned section, shows the neural network architecture for the test scenario in which 20 neurons are used as hidden layers for the four input parameters (AT, V, AP, and RH) that correspond to the output variable (EP). The Levenberg–Marquardt training algorithm involves finding dependable answers for varying numbers of hidden layers after the initial setup.

Figures 7–9 show the trained network models and their performance plots. The performance graph shows the performance of the network, which is displayed when the performance button is clicked in the training window. This enables one to know the status of the training process. While the $x$-axis indicates a number of iterations, the $y$-axis

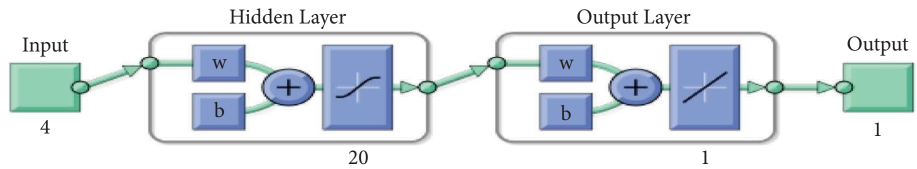


Figure 6: Neural network structure with four input parameters and 20 hidden layers.

Table 3: Dataset setting.

| | |
|---|---|
| Data size | 9568 |
| Applied variables | AT, V, AP, and RH |
| Number of neurons (hidden layer) | 20 |
| Training set size (%) | 70 |
| Validation set (%) | 15 |
| Testing set (%) | 15 |
| Training functions | LM, BR, and SCG |

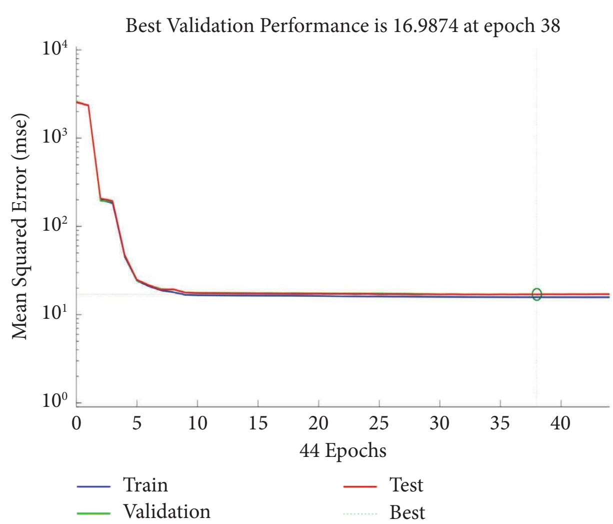


Figure 7: The LM network's optimum validation performance for 20 neurons.

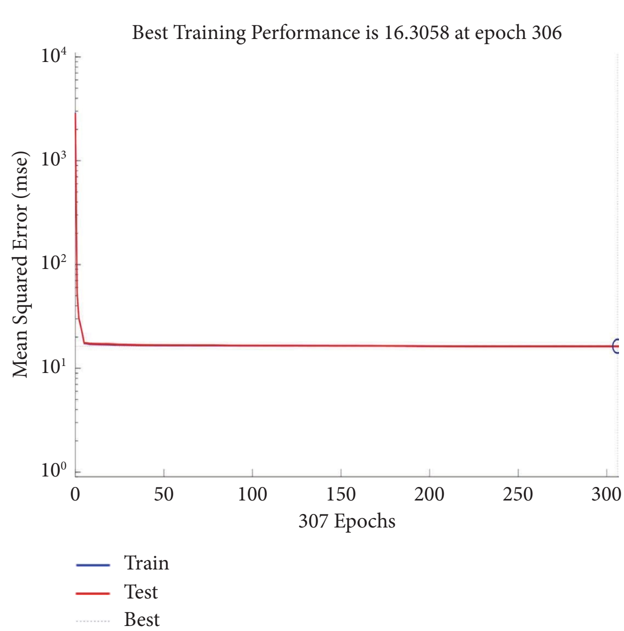


Figure 8: Optimum training performance of the BR network for 20 hidden layers.

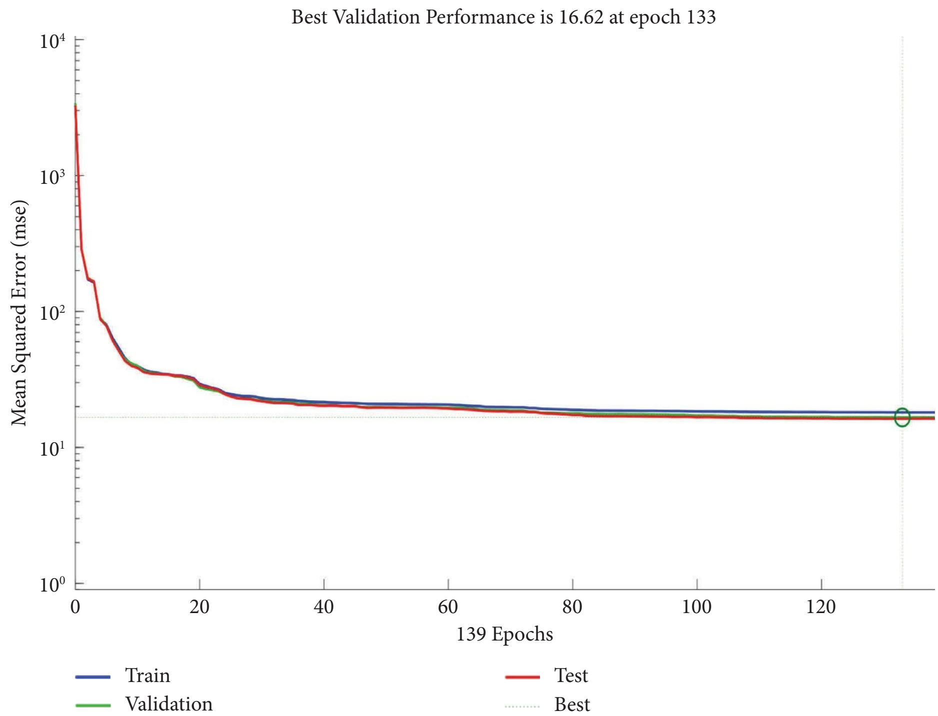


FIGURE 9: SCG network performance for 20 neurons at its best validation.

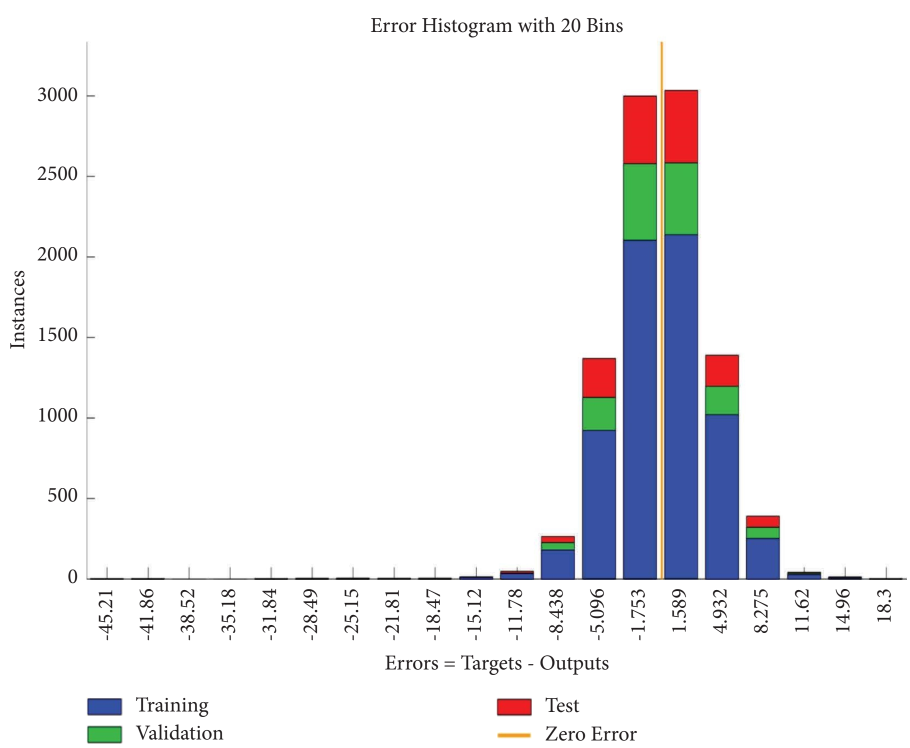


FIGURE 10: Number of instances for the LM algorithm according to the error range.

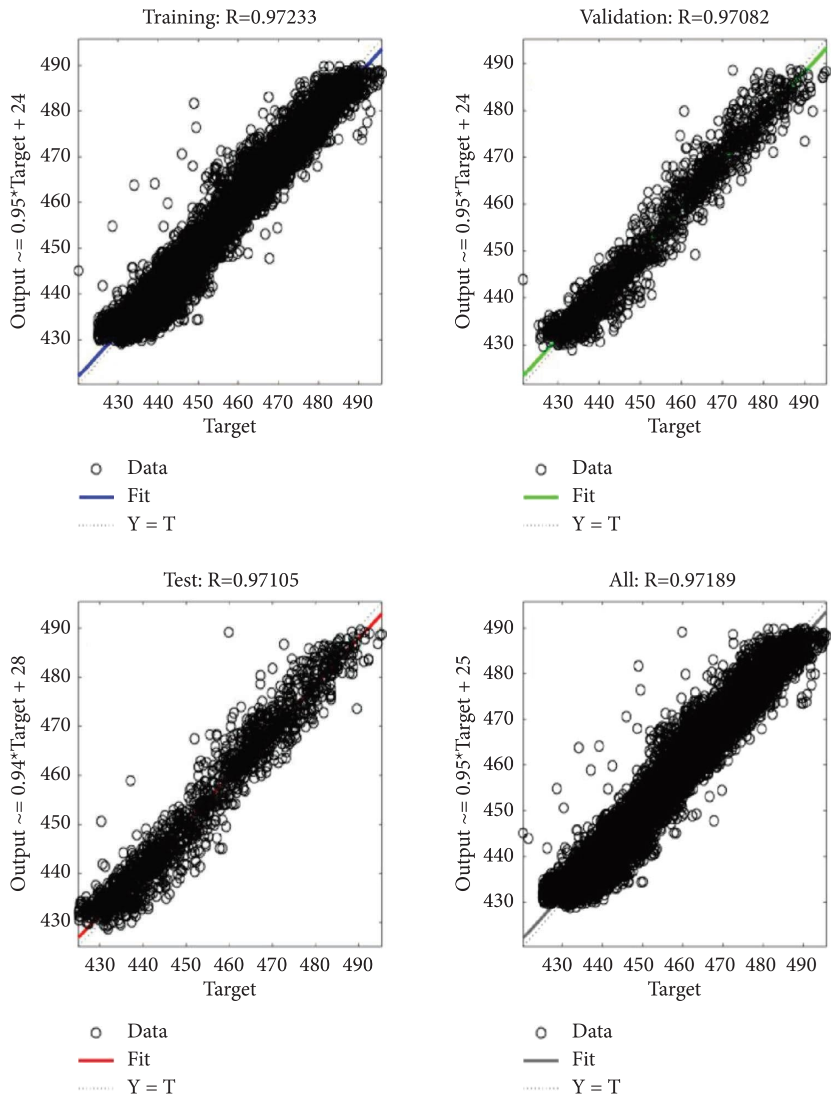


FIGURE 11: Regression analysis for the sample LM network.

TABLE 4: Hidden layers' size impact of the LM training algorithm.

| Hidden layers | Training performance | Validation performance | Training regression | Validation regression | Test regression | Stopping criterion | Iteration | Best epoch |
|---|---|---|---|---|---|---|---|---|
| 10 | 15.785 | 16.917 | 0.972 | 0.970 | 0.971 | Validation stops | 38 | 34 |
| 20 | 15.695 | 16.922 | 0.973 | 0.969 | 0.973 | Validation stops | 44 | 38 |
| 50 | 14.122 | 14.615 | 0.975 | 0.974 | 0.972 | Validation stops | 108 | 102 |
| 100 | 13.162 | 16.362 | 0.977 | 0.972 | 0.970 | Validation stops | 34 | 28 |
| 200 | 11.773 | 16.958 | 0.972 | 0.969 | 0.974 | Validation stops | 27 | 21 |
| 500 | 10.286 | 13.226 | 0.966 | 0.964 | 0.964 | Validation stops | 227 | 221 |

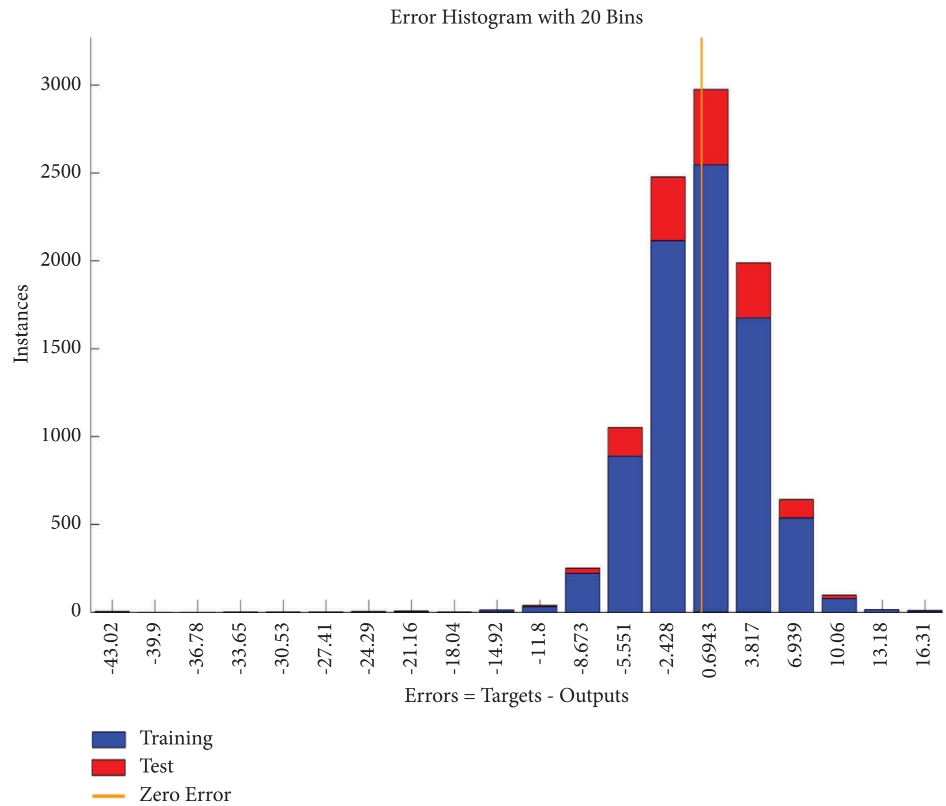


Figure 12: Number of instances of the BR algorithm according to the error range.

represents the MSE that occurred for each iteration. From the plotted line graph, the blue colour represents the training results, the green colour represents the validation results, and the red colour represents the test results. At the point when testing, training, and validation coincide, the best performance is considered to have been reached. At this point, no further training is required, and training should be stopped.

Figure 7 shows that, after 44 iterations (epochs), the 38th iteration verified the best (lowest) performance, with a mean squared error value of 16.9%.

After training, the quality of the network illustrated through the error histogram and the regression analysis is depicted in Figures 10 and 11. The discrepancies between the target and the output separated by the zero-line data are shown, presenting a small to larger divergence within the range of −11.52 to 14.96; thus, the lowest the peak, the more improved the network's performance.

The regression coefficient (correlation) for the training, validating, and testing of the entire number of data presents a very strong attitude and a high-quality network, reaching the mean value of $R = 0.972$, an almost excellent fitting ($R = 1$) between the target and the actual dataset, thus securing reliability, robustness, and good network quality.

Table 4 displays the interesting results of examining the effect on the network's quality and performance for varying numbers of neurons (hidden layers). For the lowest training and validation values, 500 neurons exhibit the best quality and network performance, while 10 neurons exhibit the worst performance.

*5.2. Bayesian Regularisation Training Algorithm.* The outcomes of the modification of the Bayesian regularisation (BR) training algorithm are shown in this section. Implementation of the Bayesian regularisation training algorithm involves the design of a network using 20 neurons (hidden layers), whereas the maximum value of the $\mu$ parameter is reached, without considering the validated data. Figure 8 shows the network's performance, with an MSE score of 16.3% at the 307th iteration, indicating excellent agreement between the training and testing data. Figure 12 depicts the error histogram and the error deviations, between −14.92 and 13.18%, ensuring improved network performance.

Figure 13 illustrates a precise fit between the target data and the output for very strong regression values ($R = 0.9716$), approaching 1. As a result, both the training samples and the tested samples show that this network quality is very good, although the validated data are not considered. The effect of the increasing number of hidden layers (neurons) on the quality is illustrated in Table 5. The performance parameter for 500 neurons provides improved outcomes, producing the poorest results for 10 neurons, with an assigned value of 13.185% for the error (MSE).

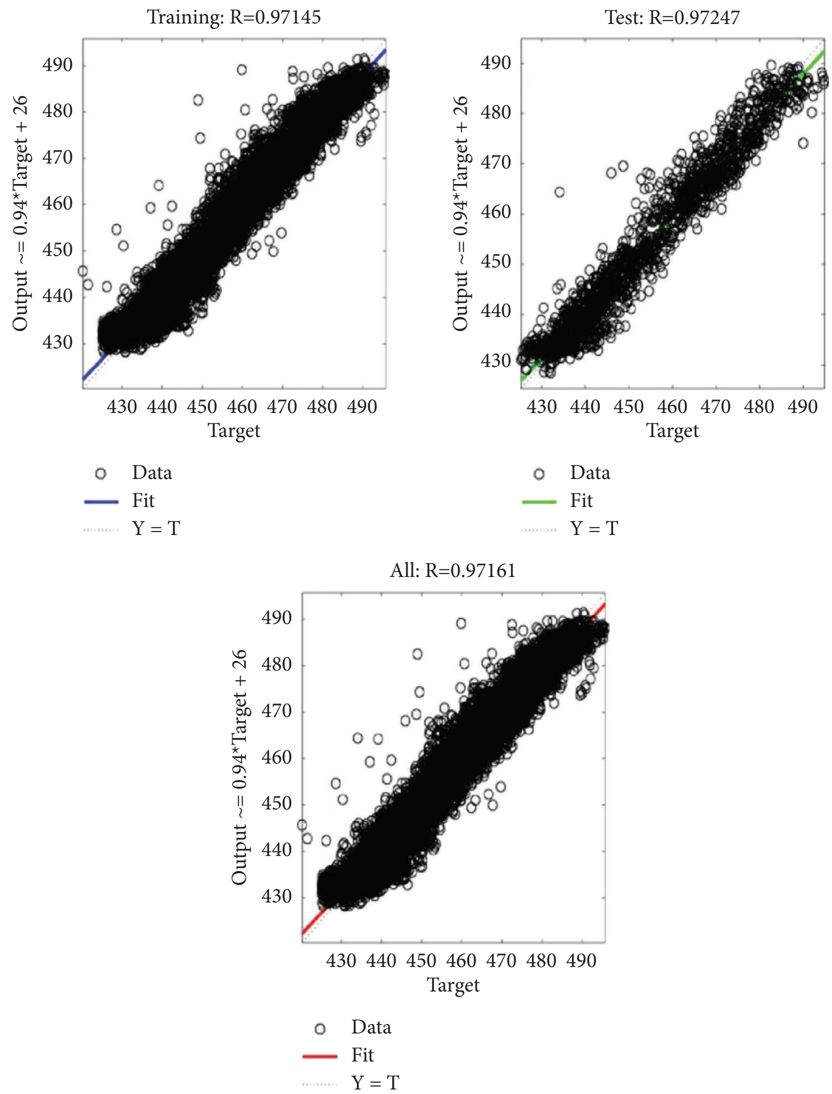


Figure 13: Regression analysis for the sample BR network.

Table 5: Hidden layers' size impact of the BR training algorithm.

| Hidden layers | Training performance | Validation performance | Training regression | Validation regression | Test regression | Stopping criterion | Iteration | Best epoch |
|---|---|---|---|---|---|---|---|---|
| 10 | 15.787 | 16.984 | 0.973 | 0.970 | 0.971 | Maximum | 307 | 306 |
| 20 | 15.294 | 16.852 | 0.974 | 0.000 | 0.973 | Maximum | 866 | 865 |
| 50 | 13.921 | 13.631 | 0.975 | 0.000 | 0.976 | Maximum epochs | 1000 | 1000 |
| 100 | 14.993 | 0.000 | 0.973 | 0.000 | 0.976 | Maximum epochs | 1000 | 1000 |
| 200 | 14.866 | 0.000 | 0.974 | 0.000 | 0.970 | Validation stops | 377 | 376 |
| 500 | 13.185 | 0.000 | 0.975 | 0.000 | 0.975 | Maximum epochs | 1000 | 1000 |

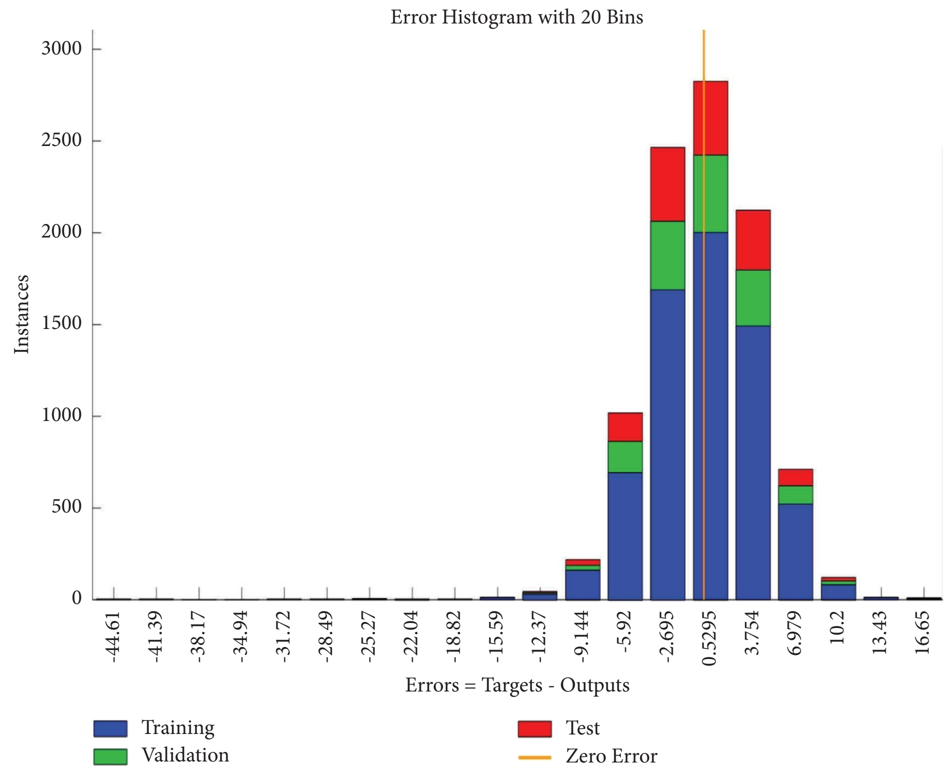


Figure 14: Number of instances with respect to the error range for the SCG training algorithm.

*5.3. Scaled Conjugate Gradient Training Algorithm.* The results of adapting the scaled conjugate gradient training algorithm at the appropriate process are covered in this section. The design process uses a sample of 20 neurons, and the best validation of the network's performance was verified after 133 iterations through 139 epochs. Figure 9 shows the assigned value of the MSE for the identical network as in the preceding two cases, which was 17.62%.

Figure 14 shows the error histogram, illustrating the error (error = target − output) via the divergent peaks' occurrence. A poor network is illustrated by the targets, showing low to high divergence for the outputs relative to the targets, compared with the other two networks, described previously.

Figure 15 illustrates a good agreement between the output and the target data for regression values ($R$) from 0.968 to 0.972, for the training, validating, and testing data, showing a good and acceptable performance, although the regression values are slightly less compared with the LM and BR structures. The main key parameter that highlights the performance of these networks is the mean squared error, and the robustness of the target versus the experimental data is expressed in terms of the regression coefficient $R$. The effect of the increasing number of neurons on the network's quality is depicted in Table 6, and outstanding solutions take place for 10 hidden layers. However, the worst solutions take place for 500 neurons and the opposite outcome occurs, compared with Tables 4 and 5.

*5.4. Comparison of the Three Training Algorithms.* The superiority of the Bayesian regularisation (BR) algorithm in terms of performance and accuracy is acknowledged reaching an improved minimum mean square value of 16.31% and an enhanced more robust regression coefficient value ($R$) of 0.972, higher than the regression values of 0.966, 0.962, and 0.959, obtained from other studies. In terms of the computational cost, the dominance of the LM algorithm after 44 simulations is identified, whilst the error histogram depicts the dominance of the Bayesian regularisation networks, due to the lowest error peak's deviation values. A considerable agreement between the BR network's advocacy, the poorness of the SCG networks, and the faster speed of LM networks is achieved with other potential investigators' performance values (MSE) of 16.75%, 16.82%, and 16.93% [3, 5, 20]. Table 7 summarises the outcomes of the three training techniques in numerical comparison used in the current study, and the physical interpretation of these results is pointed out in the succeeding section.

*5.5. Physical Interpretation of the Results.* In the present study, the pioneered approach of selecting the entire multidimensional dataset of 9568 for 70% training, 15% testing, and 15% validating provides robust and reliable outcomes, due to the initial weight's values and bias division by default randomly. This means that the training data are divided automatically (*dividerand*) and the validation error in terms

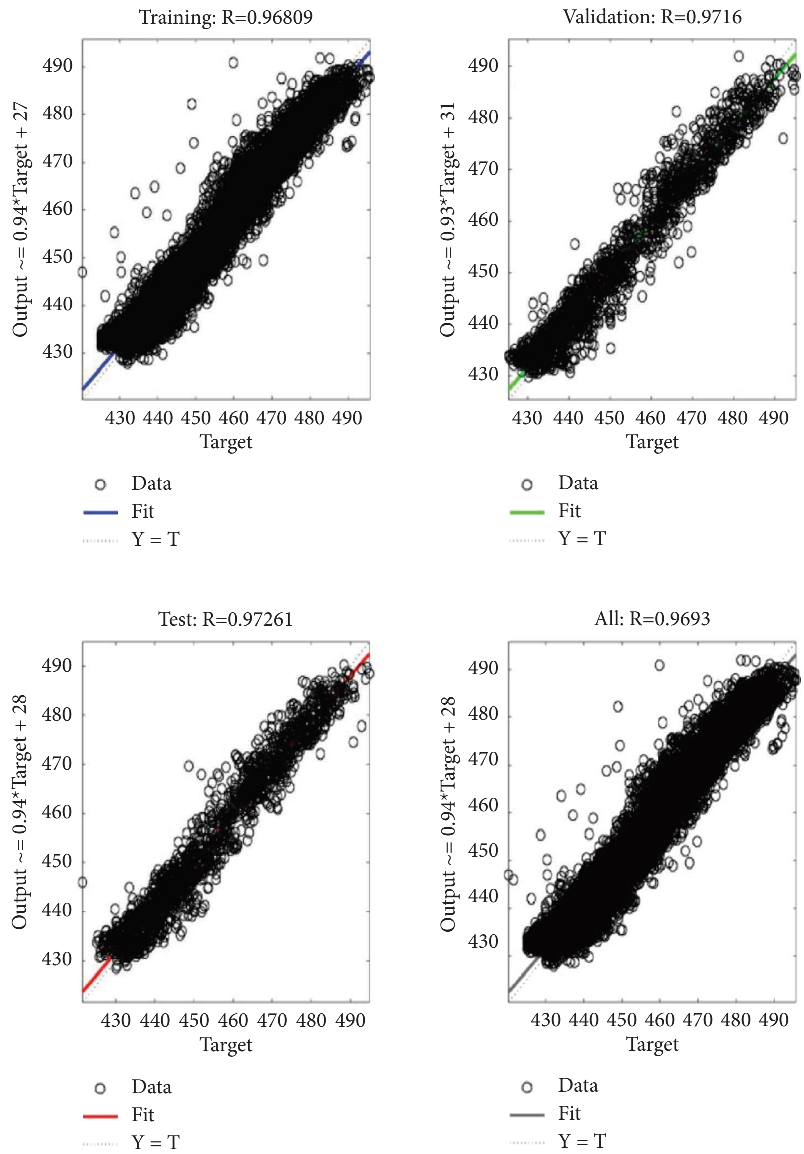


Figure 15: Regression analysis for the sample SCG network.

Table 6: Hidden layers' size impact of the SCG training algorithm.

| Hidden layers | Training performance | Validation performance | Training regression | Validation regression | Test regression | Stopping criterion | Iteration | Best epoch |
|---|---|---|---|---|---|---|---|---|
| 10 | 18.106 | 16.620 | 0.968 | 0.971 | 0.972 | Validation stops | 139 | 133 |
| 20 | 18.172 | 18.326 | 0.968 | 0.965 | 0.970 | Validation stops | 127 | 121 |
| 50 | 18.839 | 18.132 | 0.967 | 0.967 | 0.967 | Validation stops | 111 | 105 |
| 100 | 16.330 | 19.446 | 0.971 | 0.966 | 0.969 | Validation stops | 230 | 224 |
| 200 | 19.328 | 19.799 | 0.966 | 0.964 | 0.964 | Validation stops | 227 | 221 |
| 500 | 25.786 | 33.113 | 0.956 | 0.943 | 0.947 | Validation stops | 307 | 301 |

Table 7: The training algorithms' numerical comparison.

| S/N | SCG algorithm | LM algorithm | BR algorithm |
|---|---|---|---|
| 1 | After 139 iterations, the network has been trained, computationally expensive | After 44 iterations, the network has been trained, with a more beneficial computational cost | After 307 iterations, the network has been trained, most expensive computational cost |
| 2 | Highest MSE value of 17.62 | Permissible and lower MSE value of 16.92 | Optimum (lowest) MSE value of 16.3 |
| 3 | Very good regression values ($R$) of 0.970 | Better regression values ($R$) of 0.971 | More robust (higher) regression values ($R$) of 0.972 |
| 4 | Poor error histogram, due to the larger peak deviations (targets and actual data) | Satisfactory error histogram, due to lower peak deviations | Very good error histogram, due to the lowest peak deviations |

of MSE and/or RMSE (3.631) is reduced and kept at a minimum value for the increased number of hidden layers. The quality of the training process is dependent on the normalisation method, and mapping within the range from 0.01 to 0.99 is considered. The adaptation of the tan-sigmoid (*tansig*) transfer function secures robustness in the present study. The superiority of the Bayesian regularisation training algorithm compared with the Levenberg–Marquardt and the scaled conjugate gradient validates an upgraded performance for the network with the highest number of hidden layers (500) of MSE = 13.185%, and an alternative fitting (correlation) of the input and output datasets occurs at $R = 0.972$.

## 6. Conclusions

The electric power output of a 210 MW combined cycle power plant in Turkey is modelled using the regression analysis of a neural network, based on four design variables with long-term datasets over a period of six years without the use of intricate mathematical calculations and modelling. The MATLAB Neural Network Toolbox is the study's primary implementation tool with reliable settings and with very good impact on the neural network's performance. Various researchers produced interesting and reliable results for different sizes of datasets, and the novelty of this study is that it adapts the entire dataset with robust solutions with the incorporation and comparison of the three training algorithms. Therefore, for the increased size of the hidden layers, a root mean square error of 3.631% is lower than the related values of 4.17%, 4.35%, and 4.63%, as well as an improved correlation value of 0.972 compared with 0.966, 0.962, and 0.959 values obtained from other published works [3, 5, 20]. Therefore, the Levenberg–Marquardt training algorithm and the Bayesian regularisation algorithm perform better than the SCG when compared to the error rates (MSE) for the different regression coefficients (R), and BR's supremacy is attained. The improved computational cost of the simulations depicts the superiority of the LM networks.

The randomness of the ANN's model performance for each training iteration is highlighted, due to the initial weight and bias values. The increasing and different number of hidden layers does not contribute significantly to the network's quality, although the supreme-performed networks with the three different training algorithms (LM, BR, and SCG) are found for the maximum number of neurons in the present study (500), considering the superiority of the BR training algorithm of 16.31%, compared with the MSE values of 16.75%, 16.82%, and 16.93% from the literature. The importance of robust outcomes in the engineering industry is proved, by the almost excellent regression coefficients for the training, validation, and testing data ($R = 1$), in terms of a very good matching between the actual data and the target data. The "limited" capabilities of the toolbox did not provide further error analysis, and overfitting issues are not considered. Lastly, the key findings of the proposed methodology are successfully validated, showing reliable outcomes for the output electric power estimation, advocating ANN for handling massive amounts of quality datasets with faster iterations. This will contribute further to the power plant industry and other real-world applications for reliable solutions, to satisfy emerging societal needs with environmental benefits. A future study should deal with the introduction of an original error analysis methodology towards optimum performance and the coupling of stochastic techniques such as genetic algorithms for locally optimised solutions.

## Nomenclature

AI: Artificial intelligence
ANN: Artificial neural network
AP: Ambient pressure (mbar)
AT: Ambient temperature (K)
BR: Bayesian regularisation
CCHP: Combined cycle heat plant
CCGT: Combined cycle gas turbine
CCPP: Combined cycle power plant
CHP: Combined heat and power
COGAS: Combined gas air plant
HRSG: Heat recovery system generator
LM: Levenberg–Marquardt
MBE: Mean bias error (%)
MLP: Multilayer perceptron
RMSE: Root mean square error (%)
SCG: Scaled conjugate gradient.

## Data Availability

Data used for the findings of the study and simulation file are available on request.

## Conflicts of Interest

The authors declare that they have no conflicts of interest.

## Acknowledgments

The authors acknowledge Mr. Ahmad Saad for copyediting and proofreading and Ms. Svetla Meijer for advice on the editing process of the figures.

## References

[1] Iea, "Electricity, key findings," 2022, https://www.iea.org/fuels-and-technologies/electricity.
[2] C. Aurora, L. Magni, R. Scattolini, P. Colombo, F. Pretolani, and G. Villa, "Predictive control of thermal power plants," *International Journal of Robust and Nonlinear Control*, vol. 14, no. 4, pp. 415–433, 2004.
[3] E. Elfaki and A. Hassan, "Prediction of the electrical output power of combined cycle power plant using regression ANN model," *International Journal of Computer Science and Control Engineering*, vol. 6, no. 2, pp. 9–21, 2018.
[4] O. D. Jesus, M. H. Beale, B. D. Howard, and M. T. Hagan, *Neural Network Design*, Cengage Learn, Delhi, India, 2nd edition, 2014.
[5] T. k. Ibrahim, M. K. Mohammed, O. I. Awad et al., "The optimum performance of the combined cycle power plant:

a comprehensive review," *Renewable and Sustainable Energy Reviews*, vol. 79, pp. 459–474, 2017.

[6] A. Dehghani Samani, "Combined cycle power plant with indirect dry cooling tower forecasting using artificial neural network," *Decision Science Letters*, vol. 7, pp. 131–142, 2018.

[7] Y. Yoru, T. H. Karakoc, and A. Hepbasli, "Exergy analysis of a cogeneration system through artificial neural network (ANN) method," *International Journal of Exergy*, vol. 7, no. 2, pp. 178–192, 2010.

[8] M. Jefferson, P. L. Zhou, and G. Hindmarch, "Analysis by computer simulation of a combined gas turbine and steam turbine (COGAS) system for marine propulsion," *Journal of Marine Engineering & Technology*, vol. 2, no. 1, pp. 43–53, 2003.

[9] P. Hundi and R. Shahsavari, "Comparative studies among machine learning models for performance estimation and health monitoring of thermal power plants," *Applied Energy*, vol. 265, Article ID 114775, 2020.

[10] G. Ahn and S. Hur, "Continuous conditional random field model for predicting the electrical load of a combined cycle power plant," *Industrial Engineering and Management Systems*, vol. 15, no. 2, pp. 148–155, 2016.

[11] I. Lorencin, N. Andelic, V. Mrzljak, and Z. Car, "Genetic algorithm approach to design of multi-layer perceptron for combined cycle power plant electrical power output estimation," *Energies*, vol. 12, no. 22, p. 4352, 2019.

[12] Z. Qu, J. Xu, Z. Wang, R. Chi, and H. Liu, "Prediction of electricity generation from a combined cycle power plant based on a stacking ensemble and its hyperparameter optimization with a grid-search method," *Energy*, vol. 227, Article ID 120309, 2021.

[13] N. Pachauri and C. W. Ahn, "Electrical energy prediction of combined cycle power plant using gradient boosted generalized additive model," *IEEE Access*, vol. 10, pp. 24566–24577, 2022.

[14] N. S. Santarisi and S. S. Faouri, "Prediction of combined cycle power plant electrical output power using machine learning regression algorithms," *Eastern-European Journal of Enterprise Technologies*, vol. 6, no. 8 (114), pp. 16–26, 2021.

[15] R. Siddiqui, H. Anwar, F. Ullah et al., "Power prediction of combined cycle power plant (CCPP) using machine learning algorithm-based paradigm," *Wireless Communications and Mobile Computing*, vol. 2021, Article ID 9966395, 13 pages, 2021.

[16] S. A. Kalogirou, "Artificial neural networks in renewable energy systems applications: a review," *Renewable and Sustainable Energy Reviews*, vol. 5, no. 4, pp. 373–401, 2001.

[17] P. Lauret, E. Lorenz, and M. David, "Solar forecasting in a challenging insular context," *Atmosphere*, vol. 7, no. 2, pp. 18–17, 2016.

[18] D. A. Fadare, "Modelling of solar energy potential in Nigeria using an artificial neural network model," *Applied Energy*, vol. 86, no. 9, pp. 1410–1422, 2009.

[19] A. Dehghani Samani, "Combined cycle power plant with indirect dry cooling tower forecasting using artificial neural network," *Decision Science Letters*, vol. 7, no. 2, pp. 131–142, 2018.

[20] P. Tufekci, "Prediction of full load electrical power output of a base load operated combined cycle power plant using machine learning methods," *International Journal of Electrical Power & Energy Systems*, vol. 60, pp. 126–140, 2014.

[21] H. H. Erdem and S. H. Sevilgen, "Case study: effect of ambient temperature on the electricity production and fuel consumption of a simple cycle gas turbine in Turkey," *Applied Thermal Engineering*, vol. 26, no. 2-3, pp. 320–326, 2006.

[22] H. Asgari, X. Chen, M. B. Menhaj, and R. Sainudiin, "Artificial neural network-based system identification for a single-shaft gas turbine," *Journal of Engineering for Gas Turbines & Power*, vol. 135, no. 9, 2013.

[23] M. Kaiadi, "Artificial neural networks modelling for monitoring and performance analysis of a heat and power plant," M.Sc. thesis, Lund University, Sweden, Europe, 2006.

[24] H. Nikpey, M. Assadi, and P. Breuhaus, "Development of an optimized artificial neural network model for combined heat and power micro gas turbines," *Applied Energy*, vol. 108, no. C, pp. 137–148, 2013.

[25] L. X. Niu and X. J. Liu, "Multivariable generalized predictive scheme for gas turbine control in combined cycle power plant," in *Proceedings of the IEEE Conference on Cybernetics and Intelligence Systems*, pp. 791–796, Chengdu, China, September 2008.

[26] D. A. Wood, "Combined cycle gas turbine power output prediction and data mining with optimized data matching algorithm," *SN Applied Sciences*, vol. 2, no. 3, pp. 441–521, 2020.

[27] R. Manke and S. Tembhurne, "Application of back-propagation neural network to drum level control in thermal power plants," *International Journal of Computer Science Issues*, vol. 9, no. 2, pp. 520–526, 2012.

[28] S. Anvari, H. Taghavifar, R. K. Saray, S. Khalilarya, and S. Jafarmadar, "Implementation of ANN on CCHP system to predict trigeneration performance with consideration of various operative factors," *Energy Conversion and Management*, vol. 101, pp. 503–514, 2015.

[29] V. Odokwo and K. Andem, "Modeling and efficient optimization of combined gas and steam power plant using Multi-Layer Perceptron," *International Journal of Scientific Engineering and Research*, vol. 11, no. 3, pp. 827–835, 2020.

[30] K. Forderer, M. Arhens, K. Bao, I. Mauser, and H. Schmeck, "Modelling flexibility using artificial neural network," *Energy Informatics*, vol. 1, pp. 1–21, 2018.

[31] Y. D. Arferiandi, W. Caesarendra, and H. Nugraha, "Heat rate prediction of combined cycle power plant using an artificial neural network (ANN) method," *Sensors*, vol. 21, no. 4, p. 1022, 2021.

[32] F. Fantozzi and U. Desideri, "Simulation of power plant transients with artificial neural networks. Application to an existing combined cycle," *Proceedings of the Institution of Mechanical Engineers, Part A: Journal of Power and Energy*, vol. 212, no. 5, pp. 299–313, 1998.

[33] M. Fast and T. Palme, "Application of artificial neural networks to the condition monitoring and diagnosis of a combined heat and power plant," *Energy*, vol. 35, no. 2, pp. 1114–1120, 2010.

[34] M. Fast, M. Assadi, and S. De, "Development and multi-utility of an ANN model for an Industrial gas turbine," *Applied Energy*, vol. 86, no. 1, pp. 9–17, 2009.

[35] B. Akdemir, "Prediction of hourly generated electric power using artificial neural network for combined cycle power plant," *International Journal of Electrical Energy*, vol. 4, no. 2, pp. 91–95, 2016.

[36] M. N. Moqaddam and A. Sharaki, "Applying perceptron neural network in predictive of thermal power plant industry," *Researcher*, vol. 6, no. 12, pp. 49–55, 2014.

[37] R. Orosun and S. S. Adamu, "Neural network based model of an industrial oil-fired boiler system," *Nigerian Journal of Technology*, vol. 33, no. 3, pp. 293–303, 2014.

[38] T. Palmer, P. Waniczek, H. Honen, M. Assadi, and P. Jeschke, "Compressor map prediction by neural networks," *Journal of Energy and Power Engineering*, vol. 6, pp. 1651–1662, 2012.

[39] A. Rufai and H. Bashir, "Artificial neural network-based model of Ajaokuta steel power plant," *Bayero Journal of Engineering and Technology*, vol. 13, no. 2, pp. 125–134, 2018.

[40] D. Strusnik and J. Avsec, "Artificial neural networking and fuzzy logic exergy controlling model of combined heat and power system in thermal power plant," *Energy*, vol. 80, no. 1, pp. 318–330, 2015.

[41] R. Mikulandric, D. Lončar, D. Cvetinović, and G. Spiridon, "Improvement of existing coal fired thermal power plants performance by control systems modifications," *Energy*, vol. 57, pp. 55–65, 2013.

[42] I. Loboda, Y. Feldshteyn, and V. Ponomaryov, "Neural networks for gas turbine fault identification: multi-Layer Perceptron or radial basis network?" *International Journal of Turbo and Jet Engines*, vol. 29, no. 1, pp. 37–48, 2012.

[43] S. Panda, B. Swain, and S. Mishra, "Blowdown losses control in thermal power plants using neural network," *International Journal of Advancements in Research & Technology*, vol. 2, no. 5, pp. 10–13, 2013.

[44] U. Kesgin and H. Heperkan, "Simulation of thermodynamic systems using soft computing techniques," *International Journal of Energy Research*, vol. 29, no. 7, pp. 581–611, 2005.

[45] S. T. Hashemi, O. M. Ebadati E, and H. Kaur, "A hybrid conceptual cost estimating model using ANN and GA for power plant projects," *Neural Computing & Applications*, vol. 31, no. 7, pp. 2143–2154, 2019.

[46] C. A. Saleel, "Forecasting the energy output from a combined cycle thermal power plant using deep learning models," *Case Studies in Thermal Engineering*, vol. 28, Article ID 101693, 2021.

[47] S. Dutta and S. Ghosh, "Predicting electrical power output in a combined cycle power plant – a statistical approach," *International Journal of Energy Engineering*, vol. 11, no. 2, pp. 17–26, 2021.

[48] P. Kaewprapha, P. Prempaneerach, V. Singh, T. Tinikul, and N. Intarangsi, "Machine Learning approaches for estimating the efficiency of combined cycle power plant," in *Proceedings of the International Electrical Engineering Congress (iEECON)*, pp. 1–4, Khon Kaen, Thailand, March 2022.

[49] A. Lakshmanarao, G. V. Kumar, and T. S. R. Kiran, "An effective multiple linear regression model for power load prediction," *Journal of Emerging Technologies and Innovation Research*, vol. 5, no. 9, pp. 756–760, 2018.

[50] M. S. S. Danish, Z. Nazari, and T. Senjyu, "AI – coherent data – driven forecasting model for a combined cycle power plant," *Energy Conversion and Management*, vol. 286, Article ID 117063, 2023.

[51] X. Wang, X. Sun, S. Chu, J. Watada, and J. Pan, "Improved butterfly algorithm applied to prediction of combined cycle power plant," *Mathematics and Computers in Simulation*, vol. 24, pp. 337–353, 2023.

[52] T. Danesh, R. Quaret, P. Floquet, and S. Negny, "Neural network sensitivity and interpretability predictions in power plant application," 2022, https://papers.ssrn.com/sol3/papers.cfm?abstract_id=4119745.

[53] Y. Chen, X. Huang, W. Li, R. Fan, P. Zi, and X. Wang, "Application of deep learning modelling of the optimal operation conditions of auxiliary equipment of combined cycle gas turbine power station," *Energy*, vol. 285, Article ID 4449673, 2023.

[54] Y. Zhao and L. Kok Foong, "Predicting electrical power output of combined cycle power plants using a novel artificial neural network optimized by electrostatic discharge algorithm," *Measurement*, vol. 198, Article ID 111405, 2022.

[55] UCI, "UCI Machine Learning Repository: combined cycle power plant data set," 2012, https://archive.ics.uci.edu/ml/datasets/combined+cycle+power+plant.

[56] B. Alexanda Petrovic and S. Masoudi Soltani, "Optimization of post combustion CO2 capture from a combined-cycle gas turbine power plant via Taguchi design of experiment," *Processes*, vol. 7, no. 6, p. 364, 2019.

[57] M. Dirik, "Prediction of NOx emissions from gas turbines of a combined cycle power plant using an ANFIS model optimized by GA," *Fuel*, vol. 321, Article ID 124037, 2022.

[58] D. Saez, F. Milla, and L. Vargas, "Fuzzy predictive supervisory control based on genetic algorithms for gas turbines of combined cycle power plants," *IEEE Transactions on Energy Conversion*, vol. 22, no. 3, pp. 689–696, 2007.

[59] D. Sáez and R. Zuñiga, "Cluster optimization for Takagi & Sugeno fuzzy models and its application to a combined cycle power plant boiler," in *Proceedings of the 2004 American control conference*, vol. 2, pp. 1776–1781, IEEE, Boston, MA, USA, June 2004.

[60] D. S. Putra, M. Azmi, W. Muslikhin and Purwanto, and W. Purwanto, "ANN activation function comparative study for sinusoidal data," *Journal of Physics: Conference Series*, vol. 2406, no. 1, Article ID 12029, 2022.

[61] The Mathworks Inc, *MATLAB Version (R2018b)*, The MathWorks Inc, Natick, MA, USA, 2018.